Gravitasi

Subsurface Utility Mapping on STY Road Segment, Yogyakarta Using Ground Penetrating Radar (GPR) Frequency 500 Mhz

G. F. Ginting[1], P. P. Andika[1], A. Y. Paembonan[1]*

Geophysical Engineering, Sumatera Institute of Technology

Information	Abstract
	This research on the STY road segment, Yogyakarta, aimed to detect and map subsurface utilities to prevent damage during future utility installations. The study used the Ground Penetrating Radar (GPR) method with a 500 MHz frequency across 12 passes, processed with ReflexW software (version 8.2.2). Subsurface conditions were visualized in radargrams, where utilities responded with inverted V-shaped hyperbolic anomalies. Based on the radargrams, utilities consist of cables and pipes, distinguishable by their anomaly responses—cables show nested hyperbolas, while pipes exhibit single hyperbolas. A continuity of anomalies across the passes suggests a utility network. These utilities are located at depths of 0.5 m to 2.8 m, with consistent depth and dimensions supporting the interpretation of a cable and pipe network. This study provides valuable insights into subsurface utility mapping, aiding in minimizing risks during new installations.

*) e-mail: andri.paembonan@tg.itera.ac.id

1. INTRODUCTION

Infrastructure development is increasing along with increasing infrastructure needs due to population growth. Infrastructure development consists of several facilities such as electricity and clean water that require utility networks in the form of pipes and cables. Infrastructure development can lead to dense underground utility networks. Therefore, it is necessary to conduct subsurface utility mapping to prevent damage or leakage of utilities when there is a new utility planting or when pedestrian construction is carried out. Utility mapping requires detecting the position of subsurface utilities [1].

Utility mapping is a visual representation that provides information about the location of underground utilities. Utilities can be water pipes, gas pipes, electrical cables, and so on embedded underground. This mapping is very important considering the increasing infrastructure development and construction projects in the future. Utility mapping has several benefits, such as reducing losses due to damage or leakage to utilities that have been planted, can be used as a new utility planting plan when building a facility, avoiding hazards that can be caused by utility damage such as gas pipeline leaks, and so on [2]. Therefore, utility mapping is very important to support infrastructure development in the future. The method that can be used to detect subsurface utilities is the GPR method [3].

The GPR method is an active geophysical method that applies the concept of electromagnetic wave propagation to detect subsurface structures. GPR utilizes radar waves in its propagation with a frequency range of 1 - 1000 MHz [1]. The GPR method relies heavily on the electrical properties of the layer that becomes the wave propagation medium. This electrical property consists of dielectric permittivity, conductivity, and magnetic permeability of a layer [4].

The advantages of the GPR method are that it has high resolution, is non-destructive and real-time measurement. This method is widely used because it is easy to operate the tool and does not require a long time in conducting surveys. Research in GPR will produce a two-dimensional (2D) cross-section in the form of a radargram, where the presence of utility will have an anomalous hyperbole response. Hyperbolic anomalies are influenced by material from subsurface utilities [4].

In this study, the measurement location was carried out in the segment of Jalan STY, Yogyakarta. The location is one of the dense areas with infrastructure buildings in the form of residential areas and public facilities such as hospitals, offices, shops that allow for new infrastructure development in the future. The number of future infrastructure developments will cause utility development to be denser. The existence of utilities that are not mapped properly can cause damage / leakage when excavation is carried out in the planting of new utilities. This is due to the lack of information about utilities that have been planted, so research needs to be conducted to detect utilities in the area so that there is no damage to the utility network that has been built.

The conditions around the study area are paved areas and the surface is flat. This makes it difficult for the research area to be measured by other methods such as seismic, refraction and geoelectric method. This is because the geoelectric method requires a surface that can be used to plug electrodes and in

seismic space is needed to plug the geophone. This cannot be done due to paved road conditions. Conversely, the GPR method can be used easily in the area due to the flat surface, making it easier to operate the tool when surveying [5]. Therefore, the GPR method is more effectively applied to the research area.

The GPR survey in the study area used an antenna frequency of 500 MHz. This frequency is included in the high frequency so that the resolution obtained will be better. It aims to get clearer subsurface anomalies. The higher the frequency used, the shallower the depth penetration will be [6].

2. MATERIALS AND METHOD

This research was conducted on the STY Street Segment, Yogyakarta. Based on the Geological Map of Lembar Yogyakarta, Gondomanan sub-district is in the Young Merapi Volcano Sediment Formation (Qmi). The Qmi formation consists of tuff rock, volcanic ash, and lava melt [7]. In addition, around the research location there are Sentolo Formation (Tmps), Breezy Formation (Tmse), Nglanggeran Formation (Tmng), Nanggulan Formation (Teon), and Sambipitu Formation (Tmss). The regional geological map of the study area can be seen in Figure 1 [8].
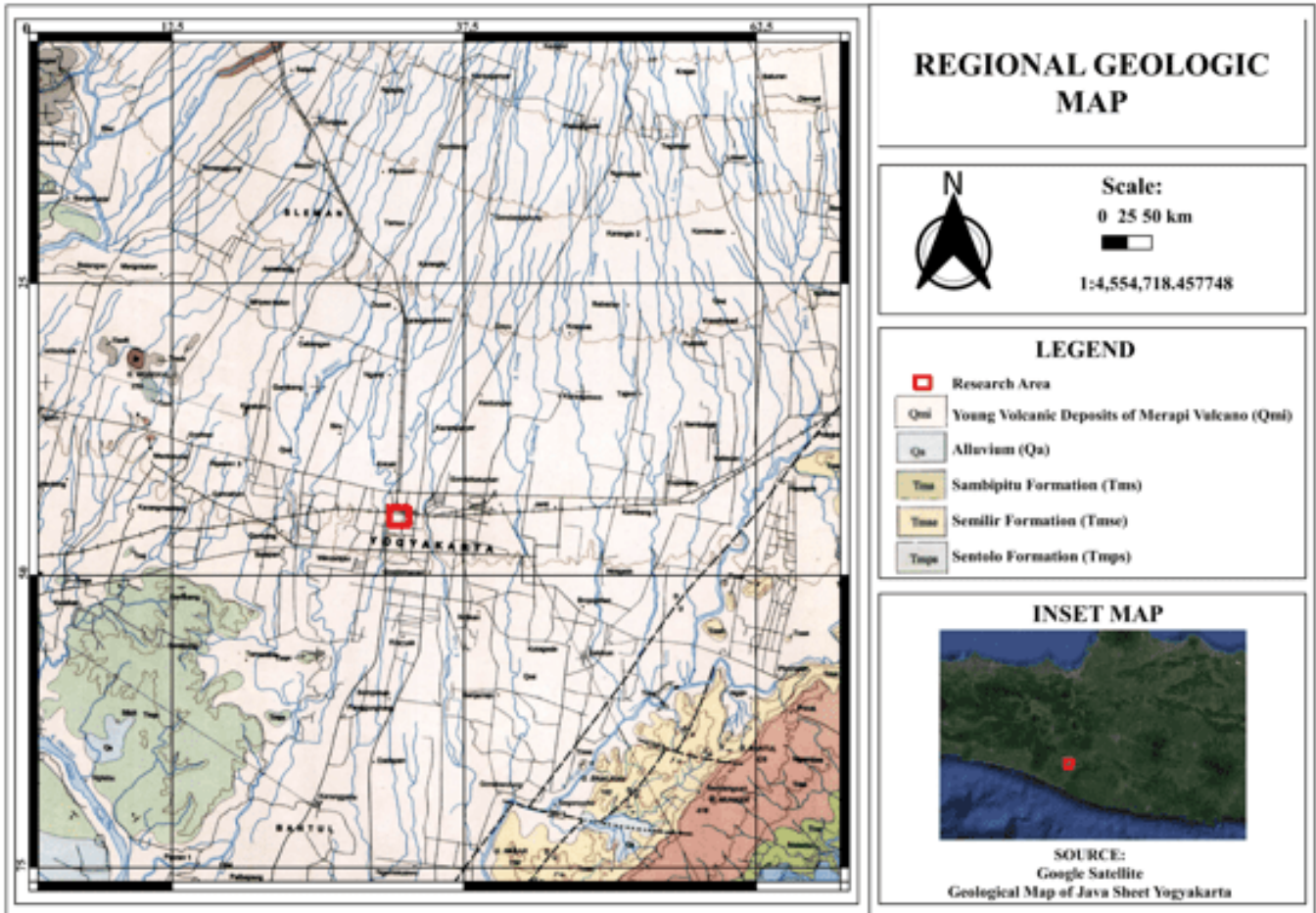
Figure 1. Regional geologic map showing the location of the study are (red rectangle), road (black line), and regional fault system (dash line) [8]

Electromagnetic waves are waves that in propagation do not require a medium. Electromagnetic waves consist of an electric field (E) and a magnetic field (H) whose propagation is perpendicular to each other, so these waves are included in transverse waves. The basic principle that explains electromagnetism is Maxwell's equation. Gauss's Law of Electricity explains the amount of electric flux that passes through a closed plane proportional to the total charge on that surface. Gauss's Law of Magnetism states that magnetism always consists of two poles, namely the north pole and the south pole. Faraday's law explains that a change in a magnetic field will produce an electric field. Ampere-Maxwell Law states that magnetic fields can be generated by electric currents and also changes in electrical shifts with respect to time [9]. The propagation of electromagnetic waves can be seen in Figure 2.
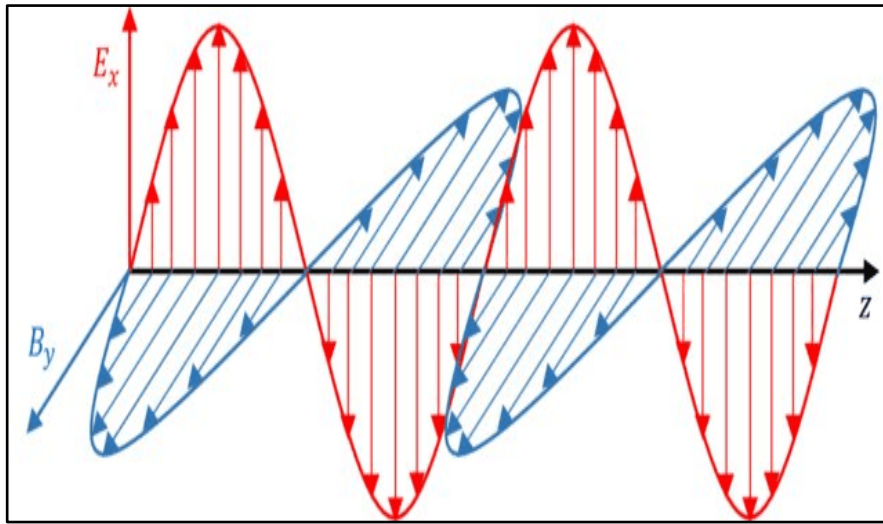
Figure 2. Curve of electromagnetic waves propagating along z line showing the electric field Ex (red curve), and magnetic field By (blue curve) [10]

The speed of electromagnetic waves in a medium can be seen in the equation (1).

$$V = \frac{\sqrt{\frac{2}{\mu\varepsilon}}}{\sqrt{1 + \sqrt{1 + \left(\frac{\sigma}{\omega\varepsilon}\right)^2}}} \qquad (1)$$

While in vacuum, the propagation speed of electromagnetic waves is c = 3×108 m/s, where the value of σ = 0, with dielectric permittivity is ε0 with magnetic permeability = μ0. On resistive medium (σ ≪ ωε) and the medium is non-magnetic (μr=1), so the speed of electromagnetic waves is obtained as in the equation (2).

$$V = \frac{1}{\sqrt{\mu\varepsilon}} = \frac{c}{\sqrt{\mu_r \varepsilon_r}} = \frac{c}{\sqrt{\varepsilon_r}} \qquad (2)$$

the higher the value of the dielectric constant (εr) of a medium, the lower the speed of electromagnetic waves. In a medium, the value of dielectric permittivity will always be greater than that of vacuum, so the value of the dielectric constant of the medium on earth will always be more than 1 [4]. The

permittivity properties of the dielectric and conductivity of the material can be seen in Table 1.

The amplitude of the wave coming with the reflected wave will be comparable as determined by the reflection coefficient (R). In radio waves, the reflection coefficient can be expressed as a function of relative permittivity on each side of the boundary plane. The reflection coefficient can be determined by:

$$R = \frac{\sqrt{\varepsilon_1} - \sqrt{\varepsilon_2}}{\sqrt{\varepsilon_1} + \sqrt{\varepsilon_2}}$$

where ε1 represents the relative permittivity of the medium carrying the incident wave and the reflected wave. The value of the reflection coefficient is -1 < R < 1. The magnitude of R determines how much the wave is reflected. If one relative permittivity across the boundary plane is much smaller than the other, then most of the wave will be reflected. The sign of the reflection coefficient determines the polarity of the reflected wave. If ε1 < ε2 the reflected wave has reverse polarity, R < 0. Whereas when ε1 > ε2 show polarity that is not reversed, R > 0.

Table 1 The dielectric constant of materials and their conductivity ([12] ; [13] ; [4])

Material	Relative Permittivity (ε_r)	Conductivity (mS/m)	V (m/ns)
Air	1,00059	0	0,3
Concrete	4 - 30	1 - 100	0,055 - 0,15
Asphalt	3 - 5	1 - 50	0,134 - 0,173
Fresh water	80	0.5	0,033
Distilled Water	80	0.1	0,033
Air Loud	80	3x10^3	0,15
PVC, epoxy, polyesters	3	-	0,173
Metal	1-2	-	-
Volcanic ash	4-7	-	0,113 - 0,15

GPR is a tool used to detect an object by utilizing electromagnetic waves, where the waves will bounce back when they hit an object. The object under study can be utilities, cables, piles, buried archaeology, ice thickness, subsidence and so on. The GPR method is a method used to detect shallow subsurface structures by utilizing a radar system which is radio waves. The important parameters in the GPR method are dielectric permittivity (ε), electrical conductivity (σ), and magnetic permeability (μ) of the medium passed because it will affect the wave propagation speed [11].

In [5], GPR consists of several components shown in Figure 3, where electromagnetic waves are emitted by the transmitter and reflected waves are received back by the receiver. Electromagnetic waves hitting the boundary plane will cause the waves to be reflected partly to the receiver and partially forwarded. Measurements with GPR are carried out with a moving tool to collect data in various places to obtain differences contained in the soil layer. The GPR system can be seen in Figure 3.
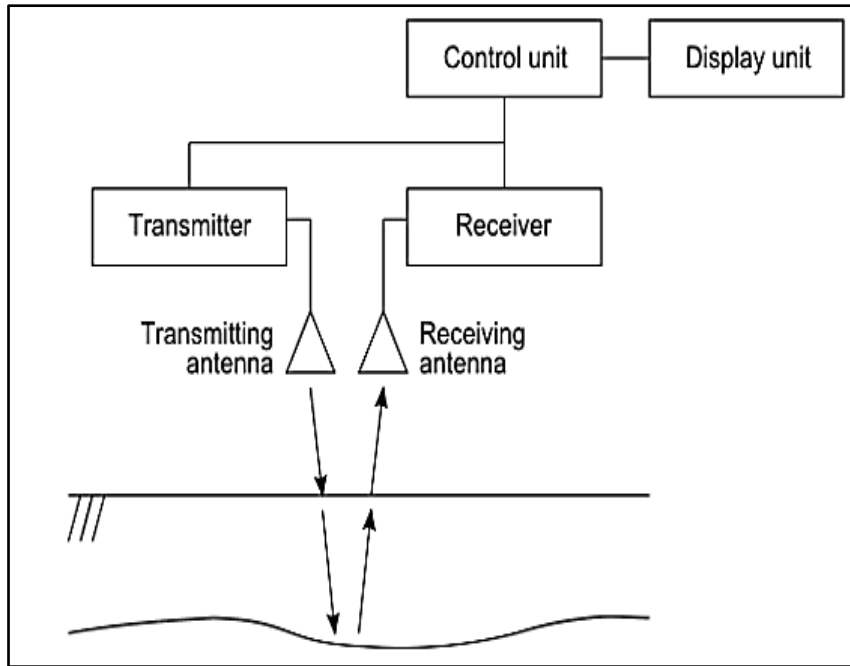
Figure 3. Block diagram of the GPR system [5]

The GPR radargram profile consists of the amplitude of the received signal against the time (T) and position (x) functions. The time axis can be converted to depth by assuming the speed of electromagnetic waves in the subsurface layers. The radargram profile can be seen in Figure 4.
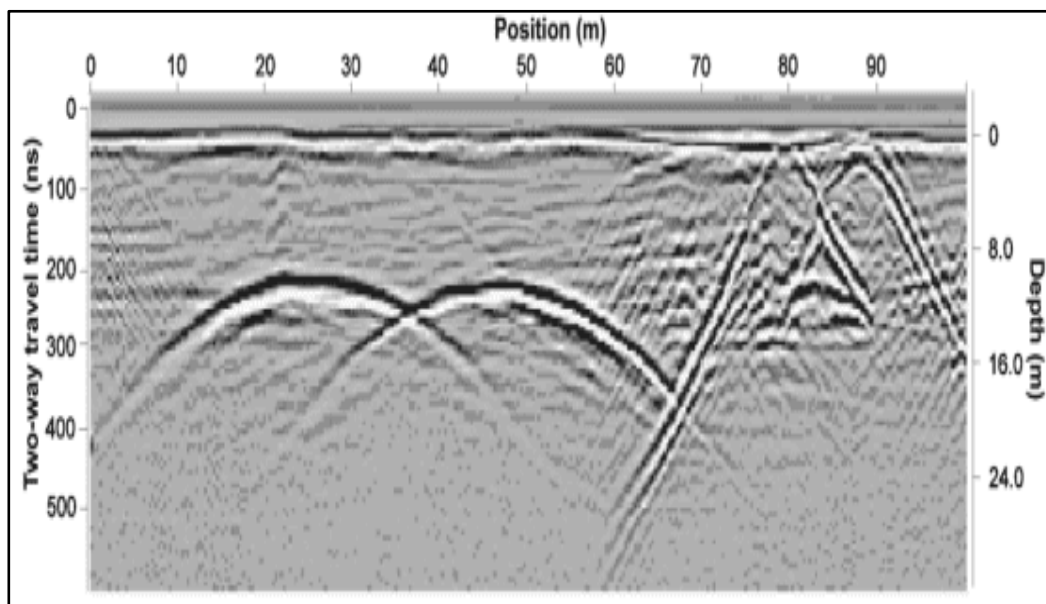
Figure 4. Example of GPR radargram profile showing the anomaly in form of curve interpreted as the utility anomaly [14]

GPR uses frequencies between 1 - 1000 MHz [4]. The use of this frequency depends on the needs when measuring it. High frequencies provide lower pulses with high time resolution and depth, but wave attenuation occurs quickly so that the penetration depth will tend to be shallower. If you use a lower frequency, the depth penetration will be deeper, but the resolution obtained will be lower [15]

In GPR systems, antennas are components that transmit and receive electromagnetic waves. The types of antennas in GPR that are often used are dipole and bowtie. Most systems consist of two antennas, one for the transmitter and one for the receiver, but the two can also be combined. Antennas with high signal gain will help improve the signal-to-noise ratio. The degree of gain of the antenna is determined by the frequency used. If the frequency used is high, the signal gain will be high. However, if the frequency used is low, it will make the system compact, but the signal gain will be lower [15].

Attenuation is the event of decreasing wave amplitude continuously as the depth of penetration increases due to the nature of the material being traversed. An illustration of attenuation of electromagnetic waves can be seen in Figure 5.
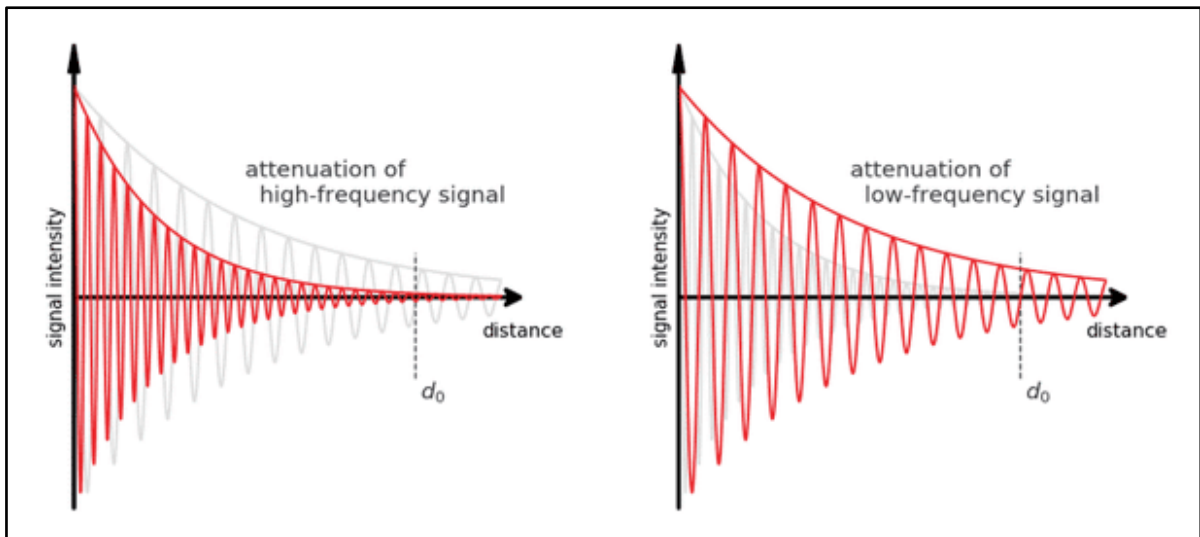
Figure 5. Attenuation of electromagnetic waves of a high frequency (left) having faster decay than lower frequency (right) [16]
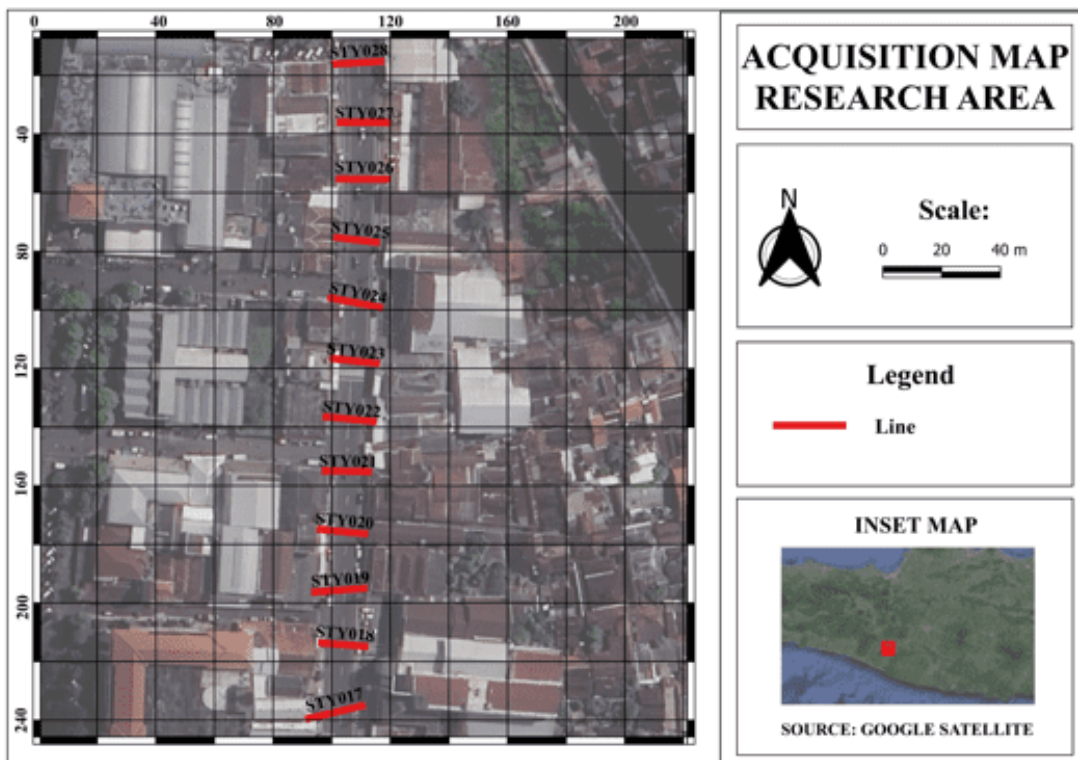
Figure 6. Map of the study area showing the acquisition line crossing the STY road

When an electromagnetic wave travels a depth of z, the attenuation coefficient (α) can be expressed as follows:

$$A = A_0 e^{-\alpha z} \ where \ \alpha \approx \begin{cases} \sqrt{\dfrac{\omega\mu\sigma}{2}} & for \ \omega\varepsilon \ll \sigma \\ \dfrac{\sigma}{2}\sqrt{\dfrac{\mu}{\varepsilon}} & for \ \sigma \ll \omega\varepsilon \end{cases} \quad (4)$$

where A0 is the initial amplitude when the wave is emitted, and A is the amplitude of the wave after propagating at depth z. When the z value $\to \infty$ then the wave amplitude will be zero [14]. Skin depth or penetration depth is the propagation distance of electromagnetic waves where the amplitude is attenuated, which is reduced by a factor of 37% of the original amplitude.

$$\delta = \frac{1}{\alpha} \quad (5)$$

$$\delta = \begin{cases} 503\sqrt{\dfrac{1}{\sigma f}} & untuk \ \omega\varepsilon \ll \sigma \\ 0{,}0053\dfrac{\sqrt{\varepsilon_r}}{\sigma} & untuk \ \sigma \ll \omega\varepsilon \end{cases} \quad (6)$$

The depth penetration will get smaller as the frequency of electromagnetic waves gets higher. The depth penetration will be higher when passing through materials with low conductivity values. When the material permittivity is high, the skin depth will be higher [14].

The research area is located in the STY Street Segment, Yogyakarta. The data consists of 12 trajectories using GPR measurements were made using Zond-12e with a frequency of 500 MHz. This measurement was carried out to detect the presence and depth of utility then utility mapping was carried out. The acquisition design of the research area can be seen in Figure 6. It shows the study site consisting of 12 passes marked with red lines. The track stretches on a paved road with a nearest track length of 13.4 meters to the farthest track of 18 meters. Measured data (raw data) must be processed to get reliable results. Several steps are performed to reduced noise and removed the effect of the measurement. Firstly, static correction aims to place the wave at the first time it arrives because of the space from the transmitting antenna (transmitter) to ground level [17]. This correction needs to be made to return the arrival time of the wave to zero (Equation 7).

$$\Delta t = t_1 - t_0 \quad (7)$$

where Δt is time difference (s), t1 presenting the picking time(s), and t0 is start time(s)

Secondly, to reduce the harmonic frequency, the Butterworth bandpass filter applied to limit the frequency. In this filter, two parameters are used, namely lower cut-off as the lower limit and upper cut-off as the upper limit of the frequency to be passed [17]. Frequency values that are outside the predetermined upper and lower limits will be considered noise so that they are eliminated [18]. Bandpass Butterworth (H(ω)) can be formulated as follows [15]:

$$H(\omega) = \frac{B^{(n)}\left(\frac{\omega}{\omega_c}\right)}{B^{(m)}\left(\frac{\omega}{\omega_c}\right)} \quad (8)$$

where Bn and Bm are orders Butterworth at-n and m respectively, ωc is a cut-off frequency, and n and m are the order of filter. This the bandpass filter is illustrated in Figure 7.
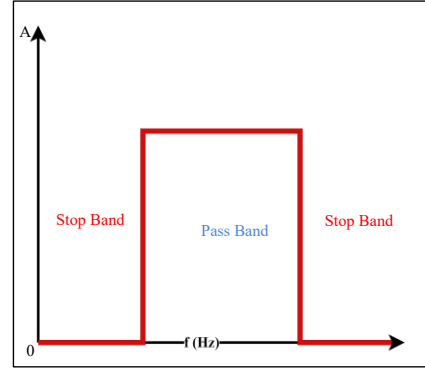
Gambar 7 Bandpass filter illustration with a low and high cut-off frequency [19]

Electromagnetic waves emitted by the transmitter will experience rapid attenuation (attenuation) of energy as depth increases, so it is necessary to do signal gain that will amplify the signal as if at every point the energy of the lomang is the same [17]. The Automatic Gain Control (AGC) multiplies the given gain value by all points on the data [18]. The gain function ($G(t)$) can be calculated as follow:

$$G(t) = d(t) \times d_{raw}(t) \quad (9)$$

where d(t) is the input gain value and draw (t) is the input raw data. Finally, processing is to smooth the signal by applying the average. Running average serves to average the noise inherent in the data. When the value used is small, it will not affect the data where there will be a lot of noise in the data. However, when using a value that is too high, the results obtained will be too smooth and eliminate target anomalies. Therefore, a median value is used to reduce noise but not eliminate target anomalies [20].

4. RESULTS AND DISCUSSION

GPR data was measured in 12 trajectories and then they are processed. The antenna frequency used is 500 MHz with a approximation depth penetration of about 4 meters. The line's length is varying from of 13.4 - 18 meters. Row data is processed including static correction, subtract-mean (dewow), gain, bandpass Butterworth, background removal, dan running average. After processing the data, the following trajectories showing the utilities anomalies indicated as pipe and cable.
Figure 8 is the result of a radargram of all trajectories that stretches. Based on the radargram, several areas have contrast amplitudes indicate that the area has different the permittivity value. The areas marked with blue squares have interpreted with a solid asphalt. In addition, hyperbole anomalies characterized by two red boxes and green boxes represent the exist underground utilities. The hyperbole in the red square is suspected as a utility in the form of a pipe while the hyperbola in the green box is suspected as a cable utility. The first pipes found at the depth between 0.5 m to 3 m, at differences distance from 0 m to 16 m of the measured lines.

The data that has been processed is the result of a GPR survey with an antenna frequency of 500 MHz on the STY road segment, Yogyakarta. The data used were 12 tracks with track lengths ranging from 13.4 - 18 meters.
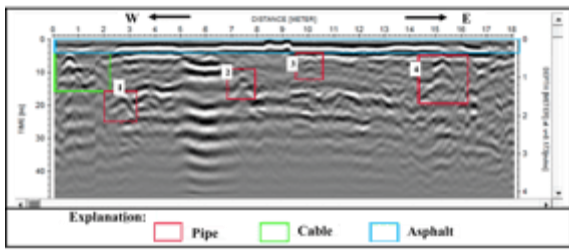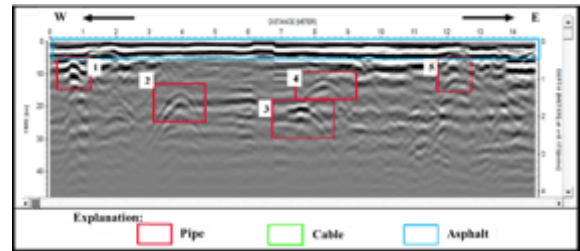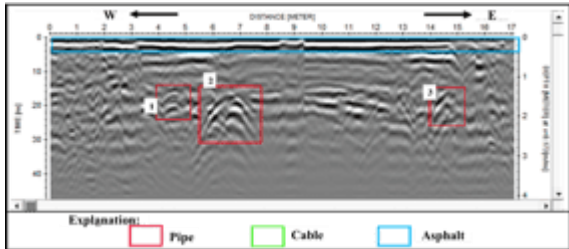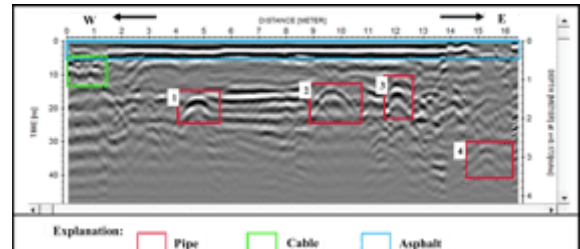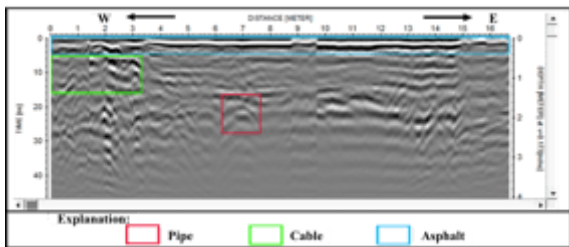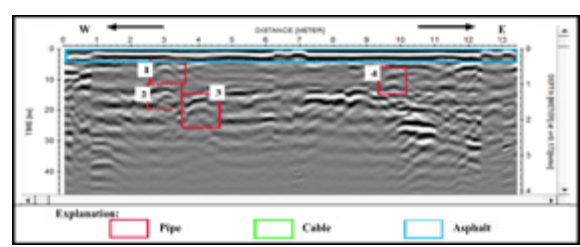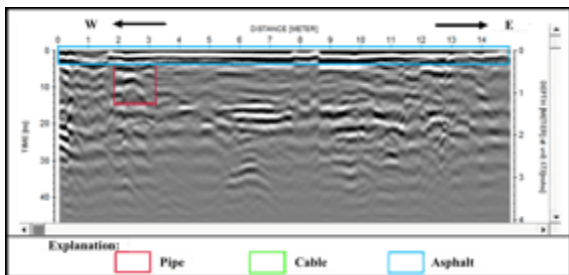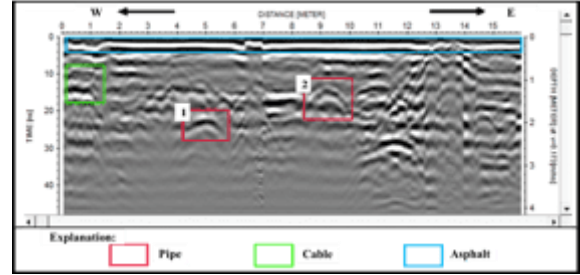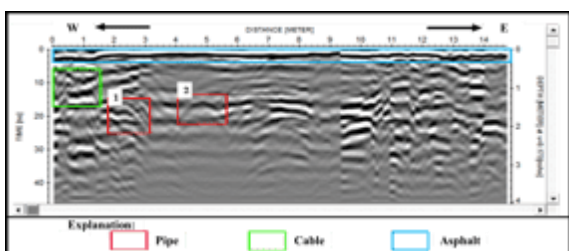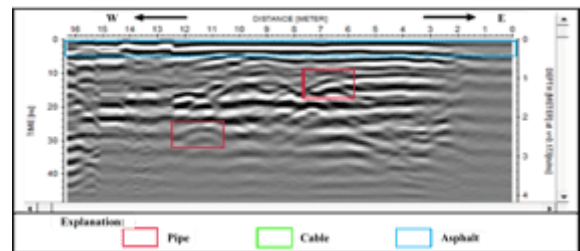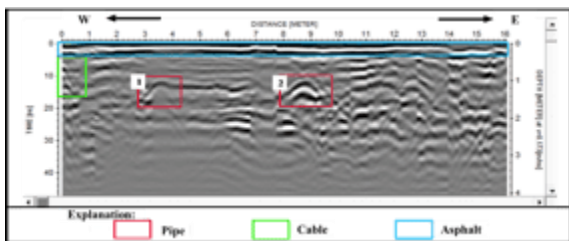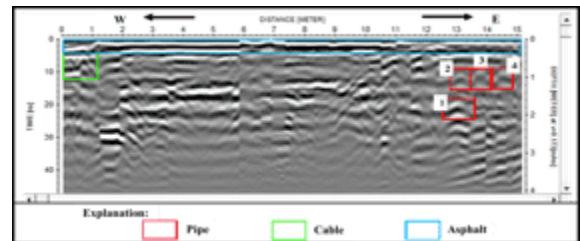
Figure 8 Processed data of 12 lines starting from STY017 (a) to line STY028 (l) showing the utility anomaly interpreted as pipe (read) cable (green) and the asphalt (blue)

The speed of electromagnetic waves is 0.173 m/ns. The speed value of electromagnetic waves is determined based on the speed value of electromagnetic waves on paved roads. This is because the condition of the study area is a paved road so that the soil under the asphalt layer has become compact due to compaction of the basic soil in the road construction process and vehicle traffic activities above the road surface [21]. The increased compactness of the soil causes the speed of electromagnetic waves in the area to be higher. The penetration depth of electromagnetic waves is 4.3 meters. The antenna frequency used includes high frequencies so that the data resolution obtained is better. This can be proven based on the processed data does not need to use many filters, but the depth penetration obtained is shallower.

Based on the radargram results from the processing of 12 passes, there are hyperbolic differences, namely single hyperbolic and stacked hyperbolic. Single hyperbolic is a pipe utility while stacked hyperbolic is a cable utility [22]. Cable utilities have a hyperbolic contrast to the ground. This is due to the high conductivity value of the object, where high conductivity will give a high reflection coefficient value so that the reflected amplitude will be high [23]. The high amplitude will give a bright / clear appearance on the radargram. While pipe utilities have a larger hyperbolic pattern than cable utilities, their color is not too contrasting with the ground because the relative permittivity value of the utility does not differ much from the soil permittivity. Therefore, such utilities can be classified as non-metallic pipes. The diameter of the pipe or cable cannot be clearly determined due to the lack of supporting data in the field. So, in this study can only be seen the difference in the dimensions of large and small hyperbolas, but the diameter of the utility cannot be determined in detail.
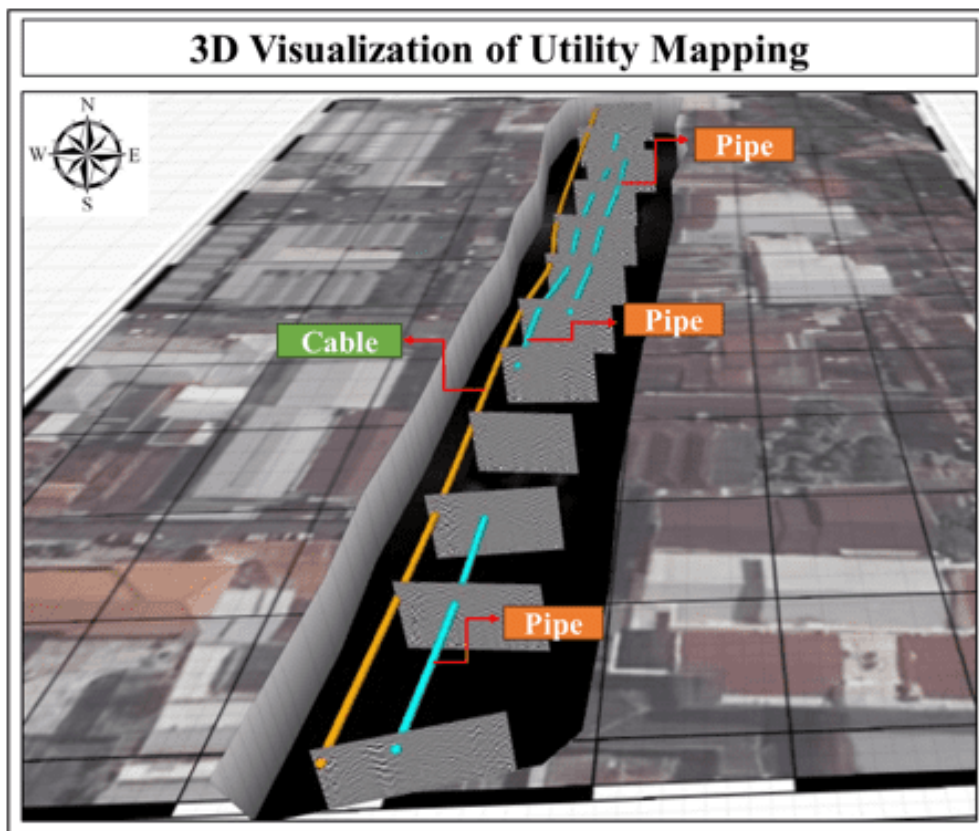
Figure 11 Visualization in 3D mode to show the continuity of the cable line and pipelines.

Of the 12 passes that have been processed, there are similarities in the utility dimension and also the amplitude and depth values are almost the same. This can be suspected as the continuity of the pipe that extends perpendicular to the direction of the trajectory. The continuity consists of cable utilities and pipeline utilities. Three-dimensional (3D) visualization of utility network on STY road segment, Yogyakarta can be seen in Figure 4.13. From the picture, there are 4 utility networks consisting of one cable network and 3 pipelines. The network is distinguished by color, which is orange which indicates cable utility while blue indicates pipelines. The cable network is located on the roadside, while the pipeline network is in the middle and also on the roadside embedded under the road body.

After finishing processing the data, picking is carried out against the peak of the hyperbole. From that point on, mapping is then carried out on the utility network that has continuity. Utility networks are marked with lines of different colors to distinguish utility networks from one another, namely orange lines indicate cable networks while blue lines indicate pipelines. The mapping can be seen in Figure 11 mapping is done between utility networks with overlays on measurement paths. The measurement path is marked with a red line.
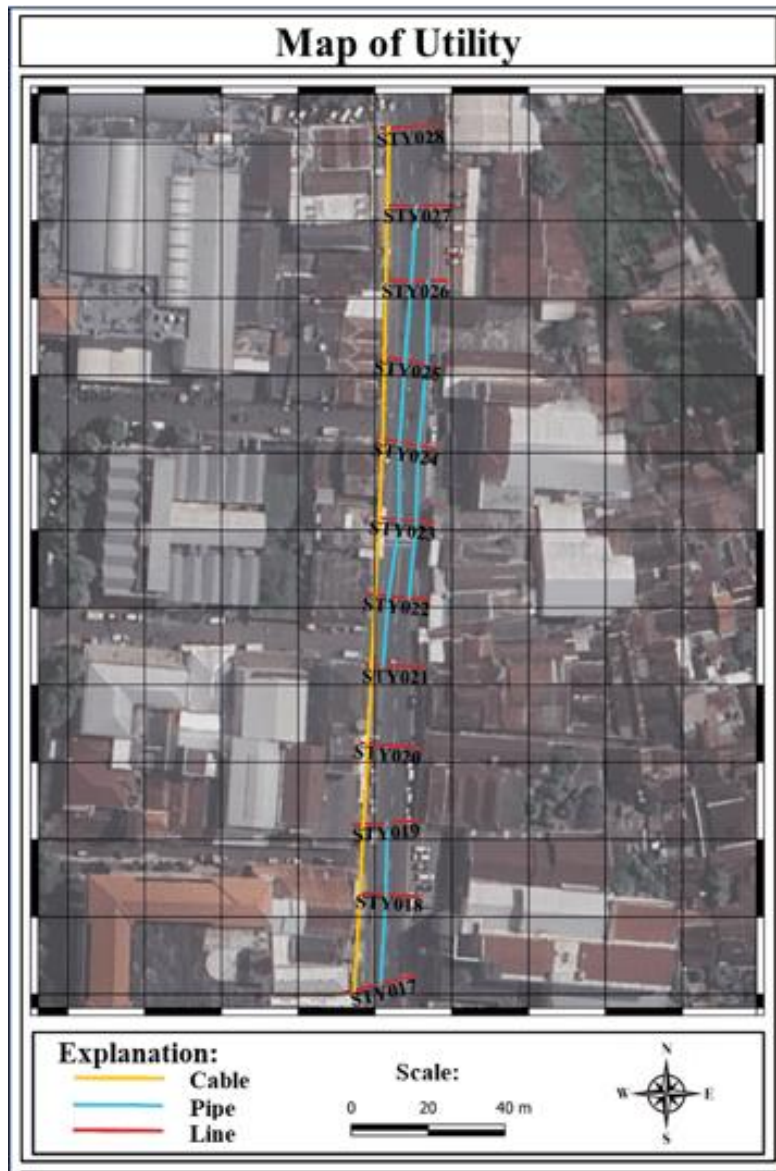
Figure 12. Utilities map on STY road segment, Yogyakarta, showing measurement line (read line) and utility lines including continuous cable line (orange line), and pipeline (blue line)

From Figure 12, the cable runs from track 17 to track 28. The first pipe near the cable runs from track 17 to track 21. The second pipe is located on track 21 to track 27. The third pipe is on tracks 22 to 26. The track length is 13.4 -18 meters, with a distance between tracks of about 20 meters. The utility is at a depth of about 0.5 – 2.8 m, but the one with continuity is at a depth of about 0.5 – 1.5 m.

4. CONCLUSION

In conclusion, the study has identified that subsurface utilities in the STY Road Segment, Yogyakarta, are located at depths between 0.5 and 3 meters showed in hyperbolic anomaly. The radargram analysis revealed five continuous features suspected to be utility networks. Single hyperbolic reflections likely represent pipe utilities, whereas stacked hyperbolic reflections are indicative of cable utilities. To enhance the visualization of the utility map, an overlay of the measurement track with the utility network was performed. This mapping shows that the pipes and cables are oriented perpendicular to the measurement trajectory. These findings provide a clear understanding of the subsurface utility layout in the studied area.

REFERENCES

1. M. Ariefa and L. Sumargana, "Penggunaan Metode Ground Penetrating Radar (GPR) Untuk Identifikasi Utilitas Bawah Tanah," Pisma Fisika, vol. 9, p. 244, 2021.

2. H. Susanto, Kajian Pemanfaatan Metode RTK Untuk Pemetaan Utilitas Jaringan Pipa Gas (Studi Kasus: PT. Perusahaan Gas Negara - SBU Wilayah II), Institut Teknologi Nasional Malang, 2012.

4. P. Sumintadireja, Geofisika Terapan untuk Geologi Eksplorasi, ITB PRESS, 2023.

5. K. Takahashi, J. Igel, H. Preetz and S. Kuroda, Problems, Perspectives and Challenges of Agricultural Water Management, Intech Open, 2012.

6. T. D. Widayanti, S. and T. Anggono, "Identifikasi Objek Bawah Permukaan Untuk Fondasi Jalan Tol di Jakarta Menggunakan Metode Ground Penetrating Radar (GPR) Pada Segmen Area Y," Al-Fiziya: Journal of Materials Science, Geophysics, Instrumentation and Theoretical Physics, vol. 3, p. 124, 2020.

7. F. K. Putri, "Karakteristik dan Potensi Mataair di Sebagian Wilayah Taman Nasional Gunung Merbabu Taman Nasional Gunung Merapi dan Sekitarnya," Jurnal INKOM, p. 44, 2017.

8. W. Rahardjo, S. and H. Rumidi, in Peta Geologi Lembar Yogyakarta, Jawa, 2012.

9. M. S. Zhdanov, Foundations of Geophysical Electromagnetic Theory and Methods, 2 ed., Candice Janco, 2018.

10. F. Khosnoud, M. B. Quadrelli, I. I. Esat and D. Robinson, "Quantum Cooperative Robotics and Autonomy," 2020.

11. J. J. Daniels, "Ground Penetrating Radar Fundamentals," Article, 2014.

12. J. M. Reynolds, An Introduction to Applied and Environmental Geophysics, 2nd Edition ed., John Wiley and Sons Ltd, 2011.

13. G. S. Baker, T. E. Jordan and J. Talley, "An Introduction to Ground Penetrating Radar (GPR)," in Baker, G.S., and Jol, H. M., eds., Stratigraphic Analyses Using GPR: Geological Society of America Special Paper 432, P, pp. 1-18, 2007.

14. P. Annan, Ground Penetrating Radar Principles, Procedures & Applications, Sensors & Software Inc., 2003.

3. G. I. "Utility Maping For Horizontal Direct Drilling (HDD) Plan," 2022. [Online]. Available: https://antesena-geosurvey.com/utility-maping-for-horizontal-direct-drilling-hdd-plan/.

15. Benedetto, F. Tosti, L. B. Ciampoli and F. D'Amico, "An Overview of Ground Penetrating Radar Signal Processing Techniques for Road Inspections," UWL Repository, 2016.

16. P. R. A. E. "Prinsip Atenuasi Sinyal Partial Discharge pada Enclosure MV Switchgear," 11 December 2020. [Online]. Available: https://www.radius.co.id/prinsip-atenuasi-sinyal-partial-discharge-pada-enclosure-mv-switchgear/. [Accessed 22 March 2024].

17. M. C. Marbun, S. and A. Rinaldi, "Identifikasi Lapisan Penyebab Longsor Menggunakan Ground Penetrating Radar Area Monumen Pesawat Sangatta (PT. Kaltim Prima Coal)," Jurnal Geosains Kutai Basin, vol. 3, 2020.

18. S. REFLEXW Version 10.4, Germany, 2024.

19. Rasyid, "Pengertian dan Cara Kerja Band Pass Filter," 8 Mei 2020. [Online]. Available: https://www.samrasyid.com/2020/05/pengertian-dan-cara-kerja-band-pass.html.

20. F. Muniiroh, "Aplikasi Metode Ground Penetrating Radar untuk Identifikasi Gua Bawah Tanah," Universitas Islam Negeri Maulana Malik Ibrahim Malang, 2020.

21. K. P. "Diklat Spesifkasi Umum Pekerjaan Jalan dan Jembatan," in Spesifikasi Pekerjaan Tanah, 2016.

22. G. Johnston, Interpreting GPR Data: The Basics. Basics of Interpreting Ground Penetrating Radar Data, Sensor & Software, 2018.

23. H. M. Jol, Ground Penetrating Radar Theory and Applications, Oxford: Elsevier Science, 2008.